Infection with CagA+ *Helicobacter pylori* induces epithelial to mesenchymal transition in human cholangiocytes

Prissadee Thanaphongdecha[1,2,3], Shannon E. Karinshak[1], Wannaporn Ittiprasert[1], Victoria H. Mann[1], Yaovalux Chamgramol[3], Chawalit Pairojkul[3], James G. Fox[4], Sutas Suttiprapa[2], Banchob Sripa [2,3,*], Paul J. Brindley[1,*]

[1] Department of Microbiology, Immunology and Tropical Medicine, and Research Center for Neglected Tropical Diseases of Poverty, School of Medicine & Health Sciences, The George Washington University, Washington DC, 20037, USA

[2] Tropical Disease Research Laboratory, Faculty of Medicine, Khon Kaen University, Khon Kaen 40002, Thailand

[3] Department of Pathology, Faculty of Medicine, Khon Kaen University, Khon Kaen, 40002, Thailand

[4] Division of Comparative Medicine, Department of Biological Engineering, Massachusetts Institute of Technology, Cambridge, 02139, MA

[*] Equal contribution

Correspondence: Paul J. Brindley, Department of Microbiology, Immunology and Tropical Medicine, and Research Center for Neglected Tropical Diseases of Poverty, School of Medicine & Health Sciences, The George Washington University, Washington DC, 20037, USA, email, pbrindley@gwu.edu; or Banchob Sripa, Tropical Disease Research Laboratory, Department of Pathology, Faculty of Medicine, Khon Kaen University, Khon Kaen 40002, Thailand, email, banchob@kku.ac.th

Abstract

Recent reports suggest that the East Asian liver fluke *Opisthorchis viverrini*, which is implicated in pathogenesis of opisthorchiasis-associated cholangiocarcinoma, serves as a reservoir of *Helicobacter pylori*. The affected cholangiocytes that line the intrahepatic biliary tract are considered to be the cell of origin of this malignancy. Here, we investigated interactions among a human cholangiocyte cell line, H69, a CCA cell line CC-LP-1, CagA+ve *Helicobacter pylori*, and *H. bilis* bacilli. Exposure to increasing numbers of *H. pylori* at 0, 1, 10,100 bacteria per cholangiocyte cell induced phenotypic changes in the cultured cholangiocytes including profusion of thread-like filopodia and loss of cell-cell contact in a dose-dependent fashion. In parallel, changes in mRNA expression followed exposure to *H. pylori*, with increased expression of epithelial to mesenchymal transition (EMT) associated-factors including snail, slug, vimentin, matrix metalloprotease, zinc finger E-box-binding homeobox, and the cancer stem cell marker CD44. Transcription levels encoding the cell adhesion marker CD24 decreased. Analysis in real time using the xCELLigence system to quantify cell proliferation, migration and invasion revealed that exposure to ten to 50 of *H. pylori* stimulated migration of H69 cells and CC-LP-1 cells, a line derived form of a human cholangiocarcinoma, and invasion through an extracellular matrix. In addition, ten bacilli of CagA+ve *H. pylori* stimulated contact-independent colony establishment in soft agar. These findings support the hypothesis that infection with *H. pylori* can contribute to the malignant transformation of the biliary epithelium.

Keyword : *Helicobacter pylori*, cholangiocyte, epithelial-to-mesenchymal transition.

Introduction

Complex associations occur between trematodes and bacterial commensals, including species capable of causing human diseases such as non-typhoidal salmonellosis, leptospirosis and Sennetsu fevers (1-3). There is increasing evidence that the East Asian liver fluke *Opisthorchis viverrini* may serve as a reservoir of *Helicobacter* and implicate *Helicobacter* in pathogenesis of opisthorchiasis-associated cholangiocarcinoma (CCA) (4-8). The International Agency for Research on Cancer of the World Health Organization classifies infection with the liver flukes *O. viverrini* and *Clonorchis sinensis* and with *H. pylori* as Group 1 carcinogens (9). In northern and northeastern Thailand and Laos, infection with *O. viverrini* is the major risk for CCA (9-12). Given the elevated prevalence of CCA in this region where infection with liver fluke prevails, and given evidence of linkages between human infection by *Helicobacter* during opisthorchiasis, these two biological carcinogens together may orchestrate the pathogenesis of opisthorchiasis and bile duct cancer. The association of *Helicobacter* and its virulence factors, including during opisthorchiasis, may underlie biliary tract disease including CCA in liver fluke-endemic regions (13). Infection with species of *Helicobacter* causes hepatobiliary tract diseases that can resemble opisthorchiasis (8, 14, 15) (16, 17). Lesions ascribed to liver fluke infection, including cholangitis, biliary hyperplasia and metaplasia, periductal fibrosis and CCA, may be due in part to *Helicobacter*-associated hepatobiliary disease.

Commensalism involving *H. pylori* and *O. viverrini* may have evolved and may facilitate conveyance of the bacillus into the human biliary tract during the migration of the juvenile fluke following ingestion of the metacercaria in raw or undercooked cyprinid fish and establishment of infection (4, 18). Since we have shown previously that curved rods resembling *Helicobacter* occur in the alimentary tract of the liver fluke (4), and given the low pH of the gut of *O. viverrini*, the *H. pylori* rods or spores might be transported by the migrating parasite. The spiral shape of *H. pylori* attach to biliary cells, which internalize in similar fashion to their behavior on gastric epithelium (19, 20).

Transition of epithelial cells to mesenchymal cells during disease and epithelial to mesenchymal transition (EMT) during development and wound healing follows conserved EMT routes with well-characterized molecular and morphological hallmarks (21). These hallmarks are clearly displayed at malignant transformation of the epithelium of the gastric mucosa resulting from infection with *H. pylori* (22). Here, we investigated interactions between CagA+ve *H. pylori*, the related species *H. bilis* (23), and human cholangiocytes including the H69 cholangiocyte cell line (24, 25) and the CCLP-1cholangiocarcinoma cell line (26). Infection with CagA+ *H. pylori* induced epithelial to mesenchymal transition in human cholangiocytes.

Materials and Methods

Cell lines of human cholangiocytes

The immortalized intrahepatic cholangiocyte cell line, H69 (24, 25), Cellosaurus (27) identifier RRID:CVCL_812,1, and the primary cholangiocarcinoma cell line, CC-LP-1 (26, 28) Cellosaurus RRID CVCL_0205, were obtained as described (26, 28-30). In brief, H69 cells were cultured in Dulbecco's Modified Eagle's Medium (DMEM) (Thermo Fisher Scientific, Inc.),

DMEM/F12 (Millipore-Sigma, St. Louis, MO) supplemented with 10% fetal bovine serum (FBS)(Invitrogen; Thermo Fisher Scientific, Inc.), supplemented with adenine, insulin, epinephrine, triiodothyronine/transferrin, hydrocortisone and epidermal growth factor and penicillin/streptomycin (PS) (all from Millipore-Sigma). CC-LP-1 cells were cultured in DMEM containing 10%FBS, L-glutamine and antibiotics, as above. Both cell lines were maintained in humidified 5% CO_2 in air at 37°C. The cells were cultured to ~80% confluence before co-culture with *H. pylori*.

Helicobacter pylori* and *Helicobacter bilis

Helicobacter pylori, ATCC 43504, isolated originally from human gastric antrum (31), and *H. bilis*, Fox *et al.* ATCC 49314, originally isolated from intestines and liver of mice (32, 33), were obtained from the American Type Culture Collection (ATCC) (Manassas, VA) and maintained on trypticase soy agar with 5% sheep blood for 72 to 96 hours (34) (Becton Dickinson, Cockeysville, MD), incubated at 37°C with gentle agitation under microaerobic conditions using the BBL Campy Pack Plus system (Becton Dickinson). After 96 hours, each species of *Helicobacter* species was harvested independently by scraping the colonies from the agar plate, the cell scraping was resuspended in DMEM/F12 medium to an optical density at 600 nm (OD_{600}) of 1.0 corresponding to ~1×10^8 colony forming units (cfu)/ml (35-37).

Morphological assessment of cholangiocytes

H. pylori was co-cultured with H69 cells at increasing multiplicities of infection (MOIs) of 0 (no bacilli), 10 and 100 for 24 hours in serum-free media. After 24 hours, the effects of *H. pylori on* H69 cell morphology were documented and images captured using an inverted microscope (Zeiss Axio Observer A1, Jena, Germany).

Cell scattering and elongation

Cells were seeded at 5×10^5 cells/well in 6-well culture plates. One day later, the cells were fed with serum- and hormone free medium in the presence of *H. pylori* at MOI of 0, 10 and 100 respectively and maintained for 24 more hours. At that interval, scattering of cells was documented using a camera fitted to an inverted microscope (Zeiss Axio Observer A1, Jena, Germany). Cell scattering was quantified by counting the total number of isolated single cells per field in ten randomly selected images at 5× magnification (modified from (38)). To assess elongation of cells, cells from ~20 randomly selected fields of view at ×20 magnification, with two to seven cells per field, were documented as above. The length to width ratio of the isolated cells was established using the ImageJ software (39).

***In vitro* wound healing assay**

Monitoring cell migration in a two-dimensional confluent monolayer in controlled *in vitro* conditions allowed investigators to simulate and explore critical mechanisms of the impact of *H. pylori* on the process of wound healing. A sheet migration approach (40, 41) was used in this study to monitor wound closure in vitro following exposure of the cholangiocytes to *H. pylori* at MOI of 0, 10 and 100. H69 cells were grown in 6-well plates (Greiner Bio-One, Monroe NC)

overnight to allow cell adherence. The cell monolayer was wounded with a thin linear scratch in the confluent cell monolayer, using a sterile 20 µl pipette tip, and the impact and wound closured monitored and measured 26 hours later, as we have described previously (29, 30). The width of the gap was measured (ImageJ software, NIH) and rate of wound closure rate compared with control cells not exposed to *H. pylori*.

Real time quantitative PCR (RT-qPCR)

Total RNA from H69 cells were extracted with RNAzolRT (Molecular Research Center, Inc., Cincinnati, OH) according to the manufacturer's instructions. The RNA quality and concentration were assessed using the NanoDrop 1000 spectrophotometer (Thermo Fisher Scientific). Total RNA (500 ng) was reversed-transcribed using iScript cDNA Synthesis Kit (Bio-Rad, Hercules, CA). Quantitative reverse transcription-polymerase chain reaction (qRT-PCR) analysis of mRNA expression of six members of the EMT-associated genes including Vimentin, Snai1, Slug, Zeb, Jam1 and MMP7; two cancer stem cells including CD44 and CD24 were undertaken on an ABI7300 system (ABI) using SsoAdvance SYBR green mixture (Bio-Rad), normalized to human GAPDH (Supplementary Table 1 provides the primer sequences). The relative fold-change was determined by the ΔΔCt method (42). Three biological replicates of the assay were undertaken.

Assessment of cell proliferation

Cell proliferation of H69 was assessed using the xCELLigence Real-time cell analyzer (RTCA) DP instrument (ACEA Biosciences, San Diego CA), as reported (29, 43, 44). H69 cells were fasted for 4 to 6 hours in 1:20 diluted medium that had been diluted 1:20 with 50% DMEM and 50% DMEM/Ham's F12, containing 1% of PS, *i.e.* 0.5% FBS final concentration, as described (45, 46), then the cells were co-cultured of viable bacilli of *H. bilis* for 120 min before starting the assay. H69 cells were harvested later using 0.25% trypsin-EDTA and washed with medium. Five thousand H69 cells were seeded on to each well of the E-plate in H69 medium and cultured for 24 hours. The culture medium was removed, and the cells were gently washed with 1×PBS. The PBS was replaced with serum diluted medium. The cellular growth was monitored in real time with readings collected at intervals of 20 minutes for ≥ 60 hours. For quantification, CI was averaged from three independent measurements at each time point.

Cell migration and invasion in response to *H. pylori*

To monitor the rate of cell migration and/or invasion in real time, we used the xCELLigence DP instrument (above) equipped with a CIM-plate 16 (ACEA Biosciences, San Diego CA), which is a 16-well Boyden chamber-like system in which each well is composed of upper and lower chambers separated by an 8-um microporous membrane (Ref). Migration/invasion was measured as the relative impedance change (cell index) across microelectronic sensors integrated into the bottom of the membrane separating the upper chamber (UC) and lower chamber (LC) of the well.

To investigate migration, H69 and CC-LP-1 cells were infected with *H. pylori* ATCC45304 strain at MOIs of 0, 1, 10, 50 and 100 respectively for 2 hours before the start of the assay, after

which the cells were harvested following treatment for 3 min with 0.25% trypsin-EDTA and washed with medium. Subsequently, 30,000 H69 or CC-LP-1 cells were seeded into each UC well in serum-free medium. Complete medium supplemented with 10 % serum was added to each LC well. Next, equilibration of the loaded CIM-plate was accomplished by incubation for 60 min to allow cell attachment, after which monitoring for migration was commenced in real time for a duration of ~100 hours with readings recorded in real time at 20 min intervals. For quantification, the cell index (CI) was averaged from three independent measurements at each time point (47).

For the invasion assay, two hours prior to conducting the assay, H69 or CC-LP-1 cells were infected with *H. pylori* ATCC45304 strain at either MOI of 0 or 10. The UC of the CIM plate was coated with a 20% solution of Matrigel™ (BD Biosciences). A total of 30,000 of H69 or CC-LP-1 cells were seeded in each well of the UC in serum-free media. H69 or CC-LP-1 medium was added as appropriate to each well of the lower chamber (LC). The loaded CIM-plate was maintained at 37$_{o}$ C in 5% CO_2 for 60 minutes to facilitate attachment of the cells. The impedance value of each well was recorded at intervals of 20 minutes for ~100 hours, at which point the experiment was terminated. The CI value provided a measurement of the rate of invasion.

Colony formation in soft agar

H69 cells were infected with *H. pylori* or *H. bilis* at MOI of 0, 10, 50 and 100 at the start of the assay. For the soft agar assay, H69 cells at 10,000 cells per well were mixed with 0.3% low melting temperature agarose (NuSieve GTG) (Lonza, Walkersville, MD) in growth medium, and plated on top of a solidified layer of 0.6% agarose in growth medium, in wells of 6- or 12-well culture plates (Greiner Bio-One). New growth medium was added every three or four days until 28 days or until the colonies had established, at which time the number of colonies of ≥ 50 µm diameter was counted and documented using an inverted microscope (48).

Statistical analysis

Differences in cell elongation, cell scattering, wound healing and colony formation among test and control groups were analysed by one-way ANOVA. Fold differences in mRNA levels, real time cell migration and invasion through extracellular matrix were analysed by two-way ANOVA followed by Dunnett's test for multiple comparisons. Analysis was accomplished using GraphPad Prism version 7 software (GraphPad, San Diego, CA). A P value of ≤ 0.05 was considered to be statistically significant.

Results

***H. pylori* induces epithelial to mesenchymal transition (EMT) in cholangiocytes**

H69 were directly exposed to increasing number of *H. pylori* at 0, 10 and 100 bacilli per cholangiocyte in 6-well plates. At 24 hours after addition of the bacilli, the normal epithelial cell appearance in tissue culture had altered to an elongated phenotype characterized by terminal thread-like filopodia and diminished cell-to-cell contacts (Figures 1,2). The extent of the

transformation was dose-dependent and, also, it indicated increased cell motility. The morphological change of H69 was quantified by measurement of the length to width ratio of the exposed cells. In a dose dependent fashion, the length: width ratio increased significantly at both MOI of and MOI of 100 when compared with MOI of 0 ($P \leq 0.01$) (Figure 2C). In addition, the numbers of isolated, single cells increased significantly in similar fashion to the increasing length: width ratio of the *H. pylori*-exposed H69 cells (Figure 2D, $P \leq 0.05$ and ≤ 0.001 at MOI 10 and 100, respectively). This phenotype resembled the 'hummingbird phenotype' displayed by the AGS gastric cell line following exposure to *H. pylori* (22). Moreover, H69 cells culture in medium supplemented with TGF-β at 5 ng/ml displayed cell aggregation and nodule formation (Figure S1).

Expression of epithelial to mesenchymal transition (EMT) associated-factors induced by exposure to *H. pylori*

The dynamic change to EMT at transcriptional level was investigated using quantitative real-time PCR of total cellular RNAs for six EMT-related factors including mesenchymal marker (vimentin), transcription factors (Snail, Slug, Zeb1), adhesion molecules (Jam1) and proteolytic enzyme (MMP7) (49). The cancer stem cell markers, CD24 and CD44 (50) were included in this analysis. Levels of the fold-difference in transcription for each of the six markers increased in a dose-dependent fashion. The regulatory transcriptional factor, Snail was markedly up-regulated with highest level of fold difference, 88-, 656- and 5,309-fold at MOI of 10, 50 and 100, respectively, followed by MMP7, with 15-, 21-, and 44-fold at MOI of 10, 50 and 100. Transcription of Slug, Zeb1, vimentin and Jam1 also was up-regulated during bacterial infection. CD24 expression was down-regulated whereas CD44 was up-regulated, revealing a $CD44^{+}$ high/$CD24^{+}$ low pattern in cells exposed to *H. pylori* (Figure 3; $P \leq 0.05$ to ≤ 0.0001 for individual EMT markers and/or MOI level as shown). A pattern of $CD44^{+}$ high/$CD24^{+}$ low expression is a hallmark biomarker of cancer stem cell activity in gastric carcinoma (50).

Exposure to *H. pylori* induces cholangiocytes to migrate, to invade extracellular matrix, and to close wounds

Analysis in real time using the CIM plates fitted to the xCELLigence system a revealed that exposure to *H. pylori* at MOI of 10 to 50 *H. pylori* stimulated significantly more migration of the H69 cholangiocytes from 24 to 96 hours from the start of real time monitoring. (Figure 4A; the graph includes *P* values at representative time points and MOI levels). The effect was not seen with MOI 100. In addition, a similar assay was undertaken using the CC-LP-1 cholangiocarcinoma cell line, but with a lower *H. pylori* MOI range. At MOI of 1, 10 and 50, *H. pylori* stimulated significantly more migration of CC-LP-1 cells from 20 to 40 hours of the real time monitoring (Figure 4B). Concerning invasion of extracellular matrix, both the CC-LP-1 and H69 cells migrated and invaded the Matrigel layer in the CIM plate at significantly higher rates than did the control cells, with significant differences evident from about 50 until 100 hours when the assay was terminated (Figure 4C, 4D). Third, scratch assays revealed two-dimensional migration of H69 cells over 24 hours. In vitro wound closure by H69 cells increased significantly to 19.47% in MOI of 10 ($P \leq 0.05$) although an effect at MOI 100 was not apparent in comparison with the control group (Figure S2).

H. pylori induces anchorage-independent colony formation

As a prospective biomarker of malignant transformation of the *Helicobacter*-infected cholangiocytes, anchorage independent colony formation by the cells was determined in a medium of soft agar. Following maintenance of the cultures for up to 28 days, counts of the numbers of colonies was revealed that a MOI of 10 *H. pylori* had induced a significant increase colony numbers of the H69 cells (Figure 5A, 5B). Significant differences from the control group were not see at MOI 50 or 100. The size of colonies also increased in all groups exposed to *H. pylori* although this was statistically significant only at the MOI of 50 (Figure S3; $P \leq 0.05$). By contrast to *H. pylori*, exposure of H69 cells to *H. bilis*, a microbe that naturally resides in the biliary tract and intestines (33, 51), decreased the number of colony formation in soft agar (Figure 5D). The ostensibly neutral or even inhibitory effect of *H. bilis* on H69 biliary cell proliferation was mirrored by inapparent increase of cellular proliferation over several days when monitored in real-time by xCELLigene using MOI of 0, 10, 50 and 100 *H. bilis* (Figure S4).

Discussion

Numerous species of *Helicobacter* have been described (52) while *H. pylori* was the first bacterial pathogen confirmed to cause gastric disease including peptic ulcer, gastric lymphoma and gastric adenocarcinoma (31, 53-56). Bacilli of *H. pylori* occur in the stomach in at least half the human population. Transmission from mother to child and by other routes takes place. The human-*H. pylori* association may be beneficial in early life, including contributions to a healthy microbiome and reduced early-onset asthma (57, 58). Many strains of *H. pylori* have been characterized at the molecular level, and these are generally classified as either CagA positive or CagA negative. The major virulence factor, cytotoxin-associated gene A (CagA) is a ~140 kDa protein encoded on the cag pathogenicity island (PAI). Cag PAI also encodes a type 4 secretion channel through which the CagA virulence factor is introduced into the host cell upon attachment by the bacillus (22). CagA locates to the cell membrane, from where it is phosphorylated by the Src kinases. Downstream of these modifications, the activated CagA orchestrates changes in morphology of the infected epithelial cell, which loses cell polarity and becomes motile, exhibiting a diagnostic 'hummingbird-like' phenotype (59-61).

The CagA oncoprotein secreted by *H. pylori* into epithelial cells is noted for its variation at the SHP2 binding site and, based on the sequence variation, is subclassified into two main types - East-Asian CagA and Western CagA. East-Asian CagA shows stronger SHP2 binding and greater biological activity than Western CagA. It has been proposed that in East Asia, the circulation of *H. pylori* strains encoding active forms of CagA underlie the elevated incidence of gastric adenocarcinoma (22).

In addition to the well-known association with gastric cancer, *H. pylori* has also been associated with hepatological disease including in the biliary tract (7, 8, 62). The related species, *H. hepaticus* and *H. bilis*, also have been associated with hepatobiliary disease (62-64). Infection with the fish-borne liver flukes *Opisthorchis viverrini*, *Clonorchis sinensis* as well as the bacterial infection with *Helicobacter pylori* are all classified as Group 1 carcinogens by the International Agency for Research on Cancer of the World Health Organization (9). Opisthorchiasis is a major risk factor for cholangiocarcinoma in the northern and northeastern

part of Thailand and Laos (9-12). In addition to gastric disease, infection with species of *Helicobacter* causes hepatobiliary tract diseases that can resemble opisthorchiasis (8, 14, 15) (16, 17). Liver fluke infection can induce lesions in biliary system including cholangitis, biliary hyperplasia and metaplasia, periductal fibrosis and CCA. These lesions derive not only from liver fluke infection but perhaps are in part the consequence of hepatobiliary tract infection with *H. pylori*. *Helicobacter* may transit from the stomach to the duodenum and enter the biliary tree through the duodenal papilla and ampulla of Vater (19, 65), and indeed may be vectored there by the liver fluke, O. viverrini ((4-6). *H. pylori*-specific DNA sequences have been detected in CCA tumors and also from lesions diagnosed as cholecystitis/cholelithiasis in regions endemic for opisthorchiasis (8, 14). Furthermore, serological findings have implicated indicate infection with *H. pylori* as a risk for CCA in Thailand (15).

Here, we investigated interactions among a human cholangiocyte cell line, H69, a CCA cell line CC-LP-1, CagA+ve *Helicobacter pylori*, and *H. bilis* bacilli. Infection of H69 with CagA+ *H. pylori* induced epithelial to mesenchymal transition phenotype in dose-dependent manner, which was characterized by cell elongation and scattering which implicate increasing change in cell motility. This phenotype of H69-infected cells was reminiscent of the modified appearance of the AGS gastric carcinoma cell after exposure *H. pylori*, which has been termed the hummingbird phenotype (66). In AGS cells, delivery of CagA by the type IV secretion mechanism from *H. pylori* to the epithelial cell subverts the normal signaling leading to actin-dependent morphological rearrangement and the hummingbird appearance. The hitherto uniform polygonal shape becomes markedly elongated with terminal needle-like projections (67).

Earlier studies in AGS cells infected with *H. pylori* had also demonstrated that the hummingbird phenotype was accompanied early on with transcription changes that reflected the epithelial to mesenchymal transition, EMT. Similar transcriptional changes were seen in the *H. pylori*-infected H69 cells. Specifically, upregulation of expression of Snai1, Slug, vimentin, Jam1, and MMP7 expression in dose-dependent fashion strongly supported, at the expression level, a dynamic change in cholangiocyte reflective of EMT. Moreover, the E-cadherin repressor, Snail was markedly up-regulated, which indicated that this factor may be a key driver of epithelial to mesenchymal transition in H69. CD44 expression was up-regulated in dose-dependent fashion, whereas CD24 decreased, showing a CD44 high/CD24 low phenotype during infection. These results indicated that *H. pylori* may not only induce EMT but also contribute to stemness and malignant transformation of the cholangiocyte.

Realtime cell monitoring approach by xCELLigence revealed that the H69 and CC-LP-1 cells showed higher cell migration when exposed to *H. pylori*. The fastest migratory rate was evident at MOI of 10, followed by MOI of 50. By contrast, the rate decreased with 100 bacteria per cell, suggesting a direct detrimental effect of exposure to elevated levels of the bacilli. Ten bacilli per cell stimulated both migration and invasion of the basement membrane model matrix by H69 and by CC-LP-1 cells, a behavioral phenotype characteristic generally of epidermal to mesenchymal transition. In addition, following exposure to *H. pylori*, H69 cells responded with an anchorage-independent cell growth in soft agar, which is an in vitro phenotype indicative of the escape from anoikosis and is characteristic of metastasis (68). The numbers of colonies of H69 cells in soft agar were significantly increased at a *H. pylori* MOI of 10. By contrast, after exposure of H69 cells to *H. bilis* in the model of contact independent cell growth and also proliferation as

quantified on the xCELLigene platform, both numbers of colonies and cell growth decreased. These responses indicated that CagA+ *H. pylori* has the potential to induce carcinogenic changes in cholangiocytes in like fashion to its carcinogenicity for the gastric epithelia.

The findings presented here conform with a malignancy-conducive relationship between the liver fluke *O. viverrini* and the bacilli *H. pylori*. By contrast, co-infections of *Helicobacter* species including *H. pylori* and some other helminths have generally been associated with diminished risk of *H. pylori*-associated gastric carcinoma (69-71). For example, the concurrent infection on mice with an intestinal nematode modulates inflammation, induces a Th2-polarizing cytokine phenotype with concurrent downmodulation of Th1 responses and the gastric immune responses, and reduces *Helicobacter*-induced gastric atrophy (72). Nonetheless, given that CagA+ *H. pylori* stimulated epithelial to mesenchymal transition of cholangiocytes which, in turn indicates the underlying mechanism of tissue fibrosis (73-75) and cancer metastasis (76-78), an explanation for why infection with the liver fluke induces bile duct cancer (79) might now be clearer – involvement by *H. pylori* and its virulence factors. *Helicobacter* likely passes from the stomach to the duodenum and enters the biliary tree through the duodenal papilla and ampulla of Vater (19, 65). To conclude, infection with CagA+ *H. pylori* induced epithelial to mesenchymal transition in human cholangiocytes, along with other changes strongly reflective of malignant transformation. Further investigation of the relationship of *O. viverrini* and *H. pylori* within the infected biliary tract clearly is warranted.

Abbreviations Cytotoxin-associated gene A (*cag*A), cholangiocarcinoma (CCA); CagA multimerization motif (CM); EMT, epithelial to mesenchymal transition; ZEB, zinc finger E-box-binding homeobox 1; VIM, vimentin; SNAII, MMP7 and cancer stem cell marker CD44; CD24.

Competing Financial Interests

The authors declare there were no competing financial interests.

Acknowledgments

P.T. acknowledges support as a PhD research scholar from the Thailand Research Fund under the Royal Golden Jubilee scholars program (grant number PHD/0013/2555); B.S. acknowledges support from Thailand Research Fund Senior Research Scholar. This work was supported by the National Health Security Office, Thailand, the Higher Education Research Promotion and National Research University Project of Thailand, Office of the Higher Education Commission, through the Health Cluster (SHeP-GMS), the Faculty of Medicine, Khon Kaen University, Thailand (award number I56110), and the Thailand Research Fund under the TRF Senior Research Scholar (RTA 5680006); the National Research Council of Thailand. The National Institute of Allergy and Infectious Diseases (NIAID), Tropical Medicine Research Center award number P50AI098639, The National Cancer Institute, award number R01CA164719, and the United States Army Medical Research and Materiel Command (USAMRMC), contract number W81XWH-12-C-0267 also provided support. The content is solely the responsibility of the authors and does not necessarily represent the official views of the funders including USAMRMC, NIAID, NCI or the NIH.

Author contributions

P.T., S.S., C.P., Y.C., J.F., B.S. and P.J.B. conceived and designed the study. P.T., S.K., V.M., W.I. performed the experiments. P.T., W.I., B.S. and PJB analyzed and interpreted the findings. P.T., B.S., W.I., S.S., and PJB wrote the manuscript. All authors read and approved the final version of the paper.

Figure legends

Figure 1. Exposure to CagA+ *H. pylori* ATCC 43504 induced morphological alteration in cholangiocytes. The photomicrographs documented cell morphology of H69 cells exposed to increasing numbers of *H. pylori* at 0, 10 and 100 bacilli per cholangiocyte, respectively (left to right) (A). The appearance of cells had changed from an epithelial to a mesenchymal phenotype including loss of cell-cell contact, elongate and spindle-shape along with growth as individual cells at after 24 hours following *H. pylori* infection in dose-dependent manner. Scale bars, 5 μm (right), 20× magnification.

Figure 2. Quantification of cell elongation of cholangiocytes upon exposure to bacilli of CagA+ *H. pylori* indicated epidermal to mesenchymal transition. The length-to-width ratio of single, isolated single cells were documented to determine cellular elongation and scattering (A, B). The number of elongated cells increased in a dose-dependent fashion in response to infection by *H. pylori* (C). By contrast, the number of isolated individual H69 cells indicated cell scattering was also significantly increased in dose-dependent fashion (D). Data are presented as the mean values with standard errors from three biological replicates. Asterisks indicates statistically significant different of *H. pylori*-infected group compared to normal group at 24 hours (*, $P \leq 0.05$; **, $P \leq 0.01$; ***, $P \leq 0.001$).

Figure 3. Transcriptional change of EMT-related and cancer stem cell marker genes after *H. pylori* exposure. Messenger RNA expression of 6 EMT-related genes and 2 cancer stem cell markers were determined with three biological replicates after 24 hours of infection. Expression of Snail, Slug, vimentin, Jam, MMP7 and CD44 increased in a dose dependently fashion whereas CD24 transcription decreased. Expression of regulatory transcriptional factor, Snail was notably up-regulated by 88-, 656- and 5,309- fold at MOI 10, 50 and 100, respectively. MMP7 expression was markedly up-regulated at each MOI. Expression of each of Slug, Zeb1, vimentin and Jam1 up-regulated in dose-dependent manner. Transcription of the cancer stem cell marker CD44 was significantly up-regulated at MOI 50 and 100 whereas CD24 was down-regulated. Together, these changes indicated that *H. pylori* could induce both EMT and stemness in human cholangiocytes. The qPCR findings were normalized to the expression levels of GAPDH in each sample.

Figure 4. Exposing cholangiocytes to *H. pylori* induced migration and invasion through extracellular matrix. H69 cholangiocytes infected with *H. pylori* migrated through Matrigel, as monitored in real time over 100 hours using CIM plates fitted to a xCELLigence DP system. Cell migration and invasion were monitored for 100 hours with chemo-attractant in the lower chamber of CIM plate. H69 cells infected with MOI 10 revealed the highest cell migration rate

followed by MOI 50 whereas MOI 100 attenuated cell migration compared with non-infected control (A). Similarly, the cholangiocarcinoma cell line, CC-LP-1 showed the highest cell migration rate when stimulated with MOI 10 followed by MOI 50. Moreover, CC-LP-1 cells significantly migrated faster even with at MOI of 1 (B). Invasion of the Matrigel extracellular matrix compared between MOI 10 and non-infected cells; invasion rates for H69 and CC-LP-1 cells significantly increased when infected (C,D).

Figure 5. Anchorage-independent cell growth in soft agar revealed cellular transformation of cholangiocytes by *H. pylori*. Representative micrographs of cholangiocyte colony appearance at day 30 exposed H69 cells (panel A, left to right). At MOI of 10, the number of colonies increased significantly ($P \leq 0.01$), but not at MOI of 50, and with a significant decrease at MOI of 100, compared with the non-infected control cells (B). By contrast, exposure of H69 cells to *H. bilis* resulted in markedly reduced numbers of colonies, in a dose-dependent fashion (C; $P \leq 0.001$). This indicated an inhibitory effect of *H. bilis* toward anchorage-independent cell growth and/or cellular transformation of human cholangiocytes (C). Three biological replicates were performed.

Supporting information

Figure S1. TGF-β promoted nodule formation. TGF-β, an EMT-stimulant, induced nodule formation of H69 cholangiocytes. Cells were cultured in the presence of 5 ng/ml TGF-β in serum- and hormone-free medium for 24 hours. Micrographs at 0 (left) and 24 (right) hours; 5×magnification.

Figure S2. Wound healing in a two-dimensional in vitro assay revealed cell migration of H69 cholangiocytes infected with *H. pylori*. Wound closure was significantly increased to 19.47% at MOI 10 of *H. pylori* ($P \leq 0.05$). An increase in wound closure was not apparent at MOI 100; 11.09% vs control, 14.47%. Micrographs at 0 (left) and 26 (right) hours; 5×magnification. the assays was performed in triplicate.

Figure S3. Size of colonies of cholangiocytes in soft agar. The colonies with diameter ≥ 50 µm were measured and counted;. mean diameters were 77.63, 91.62, 95.25 and 81.46 µm at MOI of 0, 10, 50 and 100, respectively.

Figure S4. Growth of *H. bilis* infected cholangiocytes as determined by the xCELLigence approach. H69 cells were infected with increasing number of H. bilis (ATCC 43879) at MOI of 0, 10, 50 and 100. Cell growth was inhibited when compared to the uninfected cells, at all MOIs. The +proliferation assay was performed in E-plates in minimal (serum-depleted) medium (29).

Gene name	Gen Bank Number	Primer sequence (5'-3')	Product size (bp)
CD24	NM_013230.3	Forward CACCCAGCATCCTGCTAGAC Reverse GAGACCACGAAGAGACTGGC	259
CD44	NM_00610.3	Forward GGGAGTCAAGAAGGTGGAGC Reverse CTGAGACTTGCTGGCCTCTC	237
F11r/Jam1	NM_016946.5	Forward GTGCCTACTCGGGCTTTTCT Reverse GAGCTTGACCTTGACCTCCC	201
Gapdh	NM_002046.5	Forward CCCATGTTCGTCATGGGTGT Reverse TTCTAGACGGCAGGTCAGGT	366
MMP7	NM_002423.5	Forward GGAGCTCATGGGGACTCCTA Reverse GGCCAAGTTCATGAGTTGCAG	172
Snai1	NM_005985.3	Forward AGCTCTCTGAGGCCAAGGAT Reverse GACATTCGGGAGAAGGTCCG	325
Vimentin	NM_003380.5	Forward GCAGGAGGCAGAAGAATGGT Reverse GCAGCTTCAACGGCAAAGTT	216
Zeb1	NM_001128128.2	Forward CGCAGTCTGGGTGTAATCGT Reverse CCATGCCCTGAGGAGAACTG	477

Table S1. Nucleotide sequences of primers specific for EM- associated human genes, which were used in |quantitative real-time PCR analysis.

References

1. McNulty SN, Tort JF, Rinaldi G, Fischer K, Rosa BA, Smircich P, et al. Genomes of Fasciola hepatica from the Americas Reveal Colonization with Neorickettsia Endobacteria Related to the Agents of Potomac Horse and Human Sennetsu Fevers. PLoS Genet. 2017;13(1):e1006537.
2. Van CD, Doungchawee G, Suttiprapa S, Arimatsu Y, Kaewkes S, Sripa B. Association between Opisthorchis viverrini and Leptospira spp. infection in endemic Northeast Thailand. Parasitol Int. 2017;66(4):503-9.
3. Gendrel D, Kombila M, Beaudoin-Leblevec G, Richard-Lenoble D. Nontyphoidal salmonellal septicemia in Gabonese children infected with Schistosoma intercalatum. Clin Infect Dis. 1994;18(1):103-5.
4. Deenonpoe R, Chomvarin C, Pairojkul C, Chamgramol Y, Loukas A, Brindley PJ, et al. The carcinogenic liver fluke Opisthorchis viverrini is a reservoir for species of Helicobacter. Asian Pac J Cancer Prev. 2015;16(5):1751-8.
5. Deenonpoe R, Mairiang E, Mairiang P, Pairojkul C, Chamgramol Y, Rinaldi G, et al. Elevated prevalence of Helicobacter species and virulence factors in opisthorchiasis and associated hepatobiliary disease. Sci Rep. 2017;7:42744.
6. Sripa B, Deenonpoe R, Brindley PJ. Co-infections with liver fluke and Helicobacter species: A paradigm change in pathogenesis of opisthorchiasis and cholangiocarcinoma? Parasitol Int. 2017;66(4):383-9.
7. Boonyanugomol W, Chomvarin C, Song JY, Kim KM, Kim JM, Cho MJ, et al. Effects of Helicobacter pylori gamma-glutamyltranspeptidase on apoptosis and inflammation in human biliary cells. Dig Dis Sci. 2012;57(10):2615-24.
8. Boonyanugomol W, Chomvarin C, Sripa B, Bhudhisawasdi V, Khuntikeo N, Hahnvajanawong C, et al. Helicobacter pylori in Thai patients with cholangiocarcinoma and its association with biliary inflammation and proliferation. HPB (Oxford). 2012;14(3):177-84.
9. Humans IWGotEoCRt. Biological agents. Volume 100 B. A review of human carcinogens. IARC Monogr Eval Carcinog Risks Hum. 2012;100(Pt B):1-441.
10. Sungkasubun P, Siripongsakun S, Akkarachinorate K, Vidhyarkorn S, Worakitsitisatorn A, Sricharunrat T, et al. Ultrasound screening for cholangiocarcinoma could detect premalignant lesions and early-stage diseases with survival benefits: a population-based prospective study of 4,225 subjects in an endemic area. BMC Cancer. 2016;16:346.
11. Khuntikeo N, Loilome W, Thinkhamrop B, Chamadol N, Yongvanit P. A Comprehensive Public Health Conceptual Framework and Strategy to Effectively Combat Cholangiocarcinoma in Thailand. PLoS Negl Trop Dis. 2016;10(1):e0004293.
12. Aye Soukhathammavong P, Rajpho V, Phongluxa K, Vonghachack Y, Hattendorf J, Hongvanthong B, et al. Subtle to severe hepatobiliary morbidity in Opisthorchis viverrini endemic settings in southern Laos. Acta Trop. 2015;141(Pt B):303-9.
13. Segura-Lopez FK, Guitron-Cantu A, Torres J. Association between Helicobacter spp. infections and hepatobiliary malignancies: a review. World J Gastroenterol. 2015;21(5):1414-23.
14. Boonyanugomol W, Chomvarin C, Sripa B, Chau-In S, Pugkhem A, Namwat W, et al. Molecular analysis of Helicobacter pylori virulent-associated genes in hepatobiliary patients. HPB (Oxford). 2012;14(11):754-63.
15. Pisani P, Whary MT, Nilsson I, Sriamporn S, Wadstrom T, Fox JG, et al. Cross-reactivity between immune responses to Helicobacter bilis and Helicobacter pylori in a population in

Thailand at high risk of developing cholangiocarcinoma. Clin Vaccine Immunol. 2008;15(9):1363-8.
16. Lvova MN, Tangkawattana S, Balthaisong S, Katokhin AV, Mordvinov VA, Sripa B. Comparative histopathology of Opisthorchis felineus and Opisthorchis viverrini in a hamster model: an implication of high pathogenicity of the European liver fluke. Parasitol Int. 2012;61(1):167-72.
17. Mairiang E, Laha T, Bethony JM, Thinkhamrop B, Kaewkes S, Sithithaworn P, et al. Ultrasonography assessment of hepatobiliary abnormalities in 3359 subjects with Opisthorchis viverrini infection in endemic areas of Thailand. Parasitol Int. 2012;61(1):208-11.
18. Plieskatt JL, Deenonpoe R, Mulvenna JP, Krause L, Sripa B, Bethony JM, et al. Infection with the carcinogenic liver fluke Opisthorchis viverrini modifies intestinal and biliary microbiome. FASEB J. 2013;27(11):4572-84.
19. Boonyanugomol W, Chomvarin C, Hahnvajanawong C, Sripa B, Kaparakis-Liaskos M, Ferrero RL. Helicobacter pylori cag pathogenicity island (cagPAI) involved in bacterial internalization and IL-8 induced responses via NOD1- and MyD88-dependent mechanisms in human biliary epithelial cells. PLoS One. 2013;8(10):e77358.
20. Hatakeyama M. Helicobacter pylori CagA and gastric cancer: a paradigm for hit-and-run carcinogenesis. Cell Host Microbe. 2014;15(3):306-16.
21. Lamouille S, Xu J, Derynck R. Molecular mechanisms of epithelial-mesenchymal transition. Nat Rev Mol Cell Biol. 2014;15(3):178-96.
22. Hatakeyama M. Oncogenic mechanisms of the Helicobacter pylori CagA protein. Nat Rev Cancer. 2004;4(9):688-94.
23. Fox JG. Helicobacter bilis: bacterial provocateur orchestrates host immune responses to commensal flora in a model of inflammatory bowel disease. Gut. 2007;56(7):898-900.
24. Grubman SA, Perrone RD, Lee DW, Murray SL, Rogers LC, Wolkoff LI, et al. Regulation of intracellular pH by immortalized human intrahepatic biliary epithelial cell lines. Am J Physiol. 1994;266(6 Pt 1):G1060-70.
25. Park J, Gores GJ, Patel T. Lipopolysaccharide induces cholangiocyte proliferation via an interleukin-6-mediated activation of p44/p42 mitogen-activated protein kinase. Hepatology. 1999;29(4):1037-43.
26. Shimizu Y, Demetris AJ, Gollin SM, Storto PD, Bedford HM, Altarac S, et al. Two new human cholangiocarcinoma cell lines and their cytogenetics and responses to growth factors, hormones, cytokines or immunologic effector cells. Int J Cancer. 1992;52(2):252-60.
27. Bairoch A. The Cellosaurus, a Cell-Line Knowledge Resource. J Biomol Tech. 2018;29(2):25-38.
28. Han C, Demetris AJ, Michalopoulos GK, Zhan Q, Shelhamer JH, Wu T. PPARgamma ligands inhibit cholangiocarcinoma cell growth through p53-dependent GADD45 and p21 pathway. Hepatology. 2003;38(1):167-77.
29. Smout MJ, Sotillo J, Laha T, Papatpremsiri A, Rinaldi G, Pimenta RN, et al. Carcinogenic Parasite Secretes Growth Factor That Accelerates Wound Healing and Potentially Promotes Neoplasia. PLoS Pathog. 2015;11(10):e1005209.
30. Arunsan P, Ittiprasert W, Smout MJ, Cochran CJ, Mann VH, Chaiyadet S, et al. Programmed knockout mutation of liver fluke granulin attenuates virulence of infection-induced hepatobiliary morbidity. Elife. 2019;8.
31. Marshall BJ, Warren JR. Unidentified curved bacilli in the stomach of patients with gastritis and peptic ulceration. Lancet. 1984;1(8390):1311-5.

32. Dewhirst FE, Fox JG, Mendes EN, Paster BJ, Gates CE, Kirkbride CA, et al. 'Flexispira rappini' strains represent at least 10 Helicobacter taxa. Int J Syst Evol Microbiol. 2000;50 Pt 5:1781-7.
33. Fox JG, Yan LL, Dewhirst FE, Paster BJ, Shames B, Murphy JC, et al. Helicobacter bilis sp. nov., a novel Helicobacter species isolated from bile, livers, and intestines of aged, inbred mice. J Clin Microbiol. 1995;33(2):445-54.
34. Hachem CY, Clarridge JE, Evans DG, Graham DY. Comparison of agar based media for primary isolation of Helicobacter pylori. J Clin Pathol. 1995;48(8):714-6.
35. Jung SW, Thamphiwatana S, Zhang L, Obonyo M. Mechanism of antibacterial activity of liposomal linolenic acid against Helicobacter pylori. PLoS One. 2015;10(3):e0116519.
36. Lin SN, Ayada K, Zhao Y, Yokota K, Takenaka R, Okada H, et al. Helicobacter pylori heat-shock protein 60 induces production of the pro-inflammatory cytokine IL8 in monocytic cells. J Med Microbiol. 2005;54(Pt 3):225-33.
37. Pan H, Zhang Y, He GX, Katagori N, Chen H. A comparison of conventional methods for the quantification of bacterial cells after exposure to metal oxide nanoparticles. BMC Microbiol. 2014;14:222.
38. Masuda M, Kikuchi S, Maruyama T, Sakurai-Yageta M, Williams YN, Ghosh HP, et al. Tumor suppressor in lung cancer (TSLC)1 suppresses epithelial cell scattering and tubulogenesis. J Biol Chem. 2005;280(51):42164-71.
39. Bourzac KM, Satkamp LA, Guillemin K. The Helicobacter pylori cag pathogenicity island protein CagN is a bacterial membrane-associated protein that is processed at its C terminus. Infect Immun. 2006;74(5):2537-43.
40. Bindschadler M, McGrath JL. Sheet migration by wounded monolayers as an emergent property of single-cell dynamics. J Cell Sci. 2007;120(Pt 5):876-84.
41. Liang CC, Park AY, Guan JL. In vitro scratch assay: a convenient and inexpensive method for analysis of cell migration in vitro. Nat Protoc. 2007;2(2):329-33.
42. Livak KJ, Schmittgen TD. Analysis of relative gene expression data using real-time quantitative PCR and the 2(-Delta Delta C(T)) Method. Methods. 2001;25(4):402-8.
43. Arunsan P, Chaidee A, Cochran CJ, Mann VH, Tanno T, Kumkhaek C, et al. Liver fluke granulin promotes extracellular vesicle-mediated crosstalk and cellular microenvironment conducive to cholangiocarcinoma. Neoplasia. 2020;22(5):203-16.
44. Ke N, Wang X, Xu X, Abassi YA. The xCELLigence system for real-time and label-free monitoring of cell viability. Methods Mol Biol. 2011;740:33-43.
45. Matchimakul P, Rinaldi G, Suttiprapa S, Mann VH, Popratiloff A, Laha T, et al. Apoptosis of cholangiocytes modulated by thioredoxin of carcinogenic liver fluke. Int J Biochem Cell Biol. 2015;65:72-80.
46. Rinaldi G, Yan H, Nacif-Pimenta R, Matchimakul P, Bridger J, Mann VH, et al. Cytometric analysis, genetic manipulation and antibiotic selection of the snail embryonic cell line Bge from Biomphalaria glabrata, the intermediate host of Schistosoma mansoni. Int J Parasitol. 2015;45(8):527-35.
47. Xie H, Lee L, Scicluna P, Kavak E, Larsson C, Sandberg R, et al. Novel functions and targets of miR-944 in human cervical cancer cells. Int J Cancer. 2015;136(5):E230-41.
48. Horibata S, Vo TV, Subramanian V, Thompson PR, Coonrod SA. Utilization of the Soft Agar Colony Formation Assay to Identify Inhibitors of Tumorigenicity in Breast Cancer Cells. J Vis Exp. 2015(99):e52727.

49. Zeisberg M, Neilson EG. Biomarkers for epithelial-mesenchymal transitions. J Clin Invest. 2009;119(6):1429-37.
50. Nguyen PH, Giraud J, Chambonnier L, Dubus P, Wittkop L, Belleannee G, et al. Characterization of Biomarkers of Tumorigenic and Chemoresistant Cancer Stem Cells in Human Gastric Carcinoma. Clin Cancer Res. 2017;23(6):1586-97.
51. Shomer NH, Dangler CA, Schrenzel MD, Fox JG. Helicobacter bilis-induced inflammatory bowel disease in scid mice with defined flora. Infect Immun. 1997;65(11):4858-64.
52. Flahou B, Rimbara E, Mori S, Haesebrouck F, Shibayama K. The Other Helicobacters. Helicobacter. 2015;20 Suppl 1:62-7.
53. Cover TL. Helicobacter pylori Diversity and Gastric Cancer Risk. MBio. 2016;7(1):e01869-15.
54. Marshall BJ. The pathogenesis of non-ulcer dyspepsia. Med J Aust. 1985;143(7):319.
55. Gaynor EC, Szymanski CM. The 30th anniversary of Campylobacter, Helicobacter, and Related Organisms workshops-what have we learned in three decades? Front Cell Infect Microbiol. 2012;2:20.
56. Sheh A, Fox JG. The role of the gastrointestinal microbiome in Helicobacter pylori pathogenesis. Gut Microbes. 2013;4(6):505-31.
57. Kienesberger S, Cox LM, Livanos A, Zhang XS, Chung J, Perez-Perez GI, et al. Gastric Helicobacter pylori Infection Affects Local and Distant Microbial Populations and Host Responses. Cell Rep. 2016;14(6):1395-407.
58. Cover TL, Blaser MJ. Helicobacter pylori in health and disease. Gastroenterology. 2009;136(6):1863-73.
59. Saadat I, Higashi H, Obuse C, Umeda M, Murata-Kamiya N, Saito Y, et al. Helicobacter pylori CagA targets PAR1/MARK kinase to disrupt epithelial cell polarity. Nature. 2007;447(7142):330-3.
60. Hatakeyama M, Higashi H. Helicobacter pylori CagA: a new paradigm for bacterial carcinogenesis. Cancer Sci. 2005;96(12):835-43.
61. Yamaoka Y. Mechanisms of disease: Helicobacter pylori virulence factors. Nat Rev Gastroenterol Hepatol. 2010;7(11):629-41.
62. Murphy G, Michel A, Taylor PR, Albanes D, Weinstein SJ, Virtamo J, et al. Association of seropositivity to Helicobacter species and biliary tract cancer in the ATBC study. Hepatology. 2014;60(6):1963-71.
63. Mateos-Munoz B, Perez-de-la-Serna J, Ruiz-de-Leon A, Serrano-Falcon B, Casabona-Frances S, Velasco-Cerrudo A, et al. Enterohepatic Helicobacter other than Helicobacter pylori. Rev Esp Enferm Dig. 2013;105(8):477-84.
64. Zhou D, Wang JD, Weng MZ, Zhang Y, Wang XF, Gong W, et al. Infections of Helicobacter spp. in the biliary system are associated with biliary tract cancer: a meta-analysis. Eur J Gastroenterol Hepatol. 2013;25(4):447-54.
65. Pellicano R, Menard A, Rizzetto M, Megraud F. Helicobacter species and liver diseases: association or causation? Lancet Infect Dis. 2008;8(4):254-60.
66. Wroblewski LE, Peek RM, Jr., Wilson KT. Helicobacter pylori and gastric cancer: factors that modulate disease risk. Clin Microbiol Rev. 2010;23(4):713-39.
67. Segal ED, Cha J, Lo J, Falkow S, Tompkins LS. Altered states: involvement of phosphorylated CagA in the induction of host cellular growth changes by Helicobacter pylori. Proc Natl Acad Sci U S A. 1999;96(25):14559-64.

68. Simpson CD, Anyiwe K, Schimmer AD. Anoikis resistance and tumor metastasis. Cancer Lett. 2008;272(2):177-85.
69. Holcombe C. Helicobacter pylori: the African enigma. Gut. 1992;33(4):429-31.
70. Du Y, Agnew A, Ye XP, Robinson PA, Forman D, Crabtree JE. Helicobacter pylori and Schistosoma japonicum co-infection in a Chinese population: helminth infection alters humoral responses to H. pylori and serum pepsinogen I/II ratio. Microbes Infect. 2006;8(1):52-60.
71. Whary MT, Sundina N, Bravo LE, Correa P, Quinones F, Caro F, et al. Intestinal helminthiasis in Colombian children promotes a Th2 response to Helicobacter pylori: possible implications for gastric carcinogenesis. Cancer Epidemiol Biomarkers Prev. 2005;14(6):1464-9.
72. Fox JG, Beck P, Dangler CA, Whary MT, Wang TC, Shi HN, et al. Concurrent enteric helminth infection modulates inflammation and gastric immune responses and reduces helicobacter-induced gastric atrophy. Nat Med. 2000;6(5):536-42.
73. Fragiadaki M, Mason RM. Epithelial-mesenchymal transition in renal fibrosis - evidence for and against. Int J Exp Pathol. 2011;92(3):143-50.
74. Rout-Pitt N, Farrow N, Parsons D, Donnelley M. Epithelial mesenchymal transition (EMT): a universal process in lung diseases with implications for cystic fibrosis pathophysiology. Respir Res. 2018;19(1):136.
75. Stone RC, Pastar I, Ojeh N, Chen V, Liu S, Garzon KI, et al. Epithelial-mesenchymal transition in tissue repair and fibrosis. Cell Tissue Res. 2016;365(3):495-506.
76. Kalluri R, Weinberg RA. The basics of epithelial-mesenchymal transition. J Clin Invest. 2009;119(6):1420-8.
77. Li L, Li W. Epithelial-mesenchymal transition in human cancer: comprehensive reprogramming of metabolism, epigenetics, and differentiation. Pharmacol Ther. 2015;150:33-46.
78. Sciacovelli M, Frezza C. Metabolic reprogramming and epithelial-to-mesenchymal transition in cancer. FEBS J. 2017;284(19):3132-44.
79. Jurberg AD, Brindley PJ. Gene function in schistosomes: recent advances toward a cure. Front Genet. 2015;6:144.

Figure 1

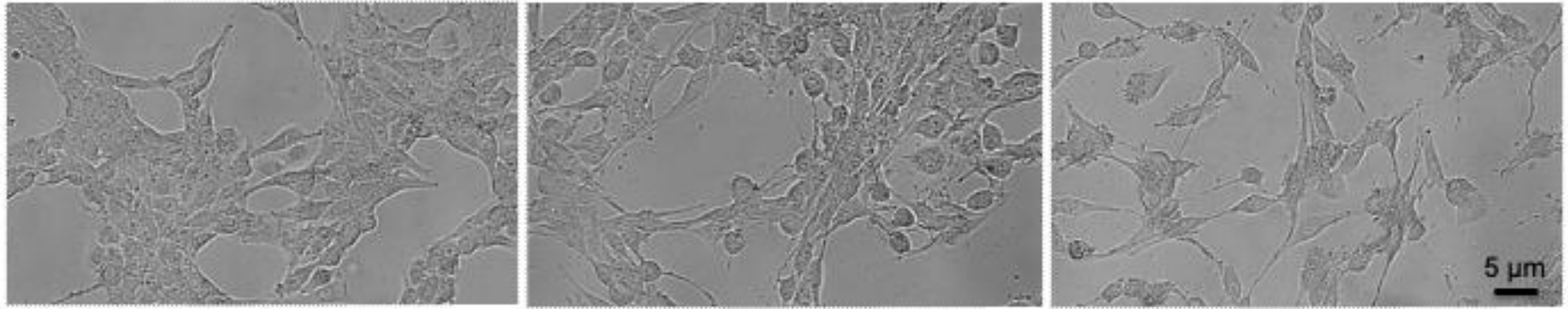

Figure 2

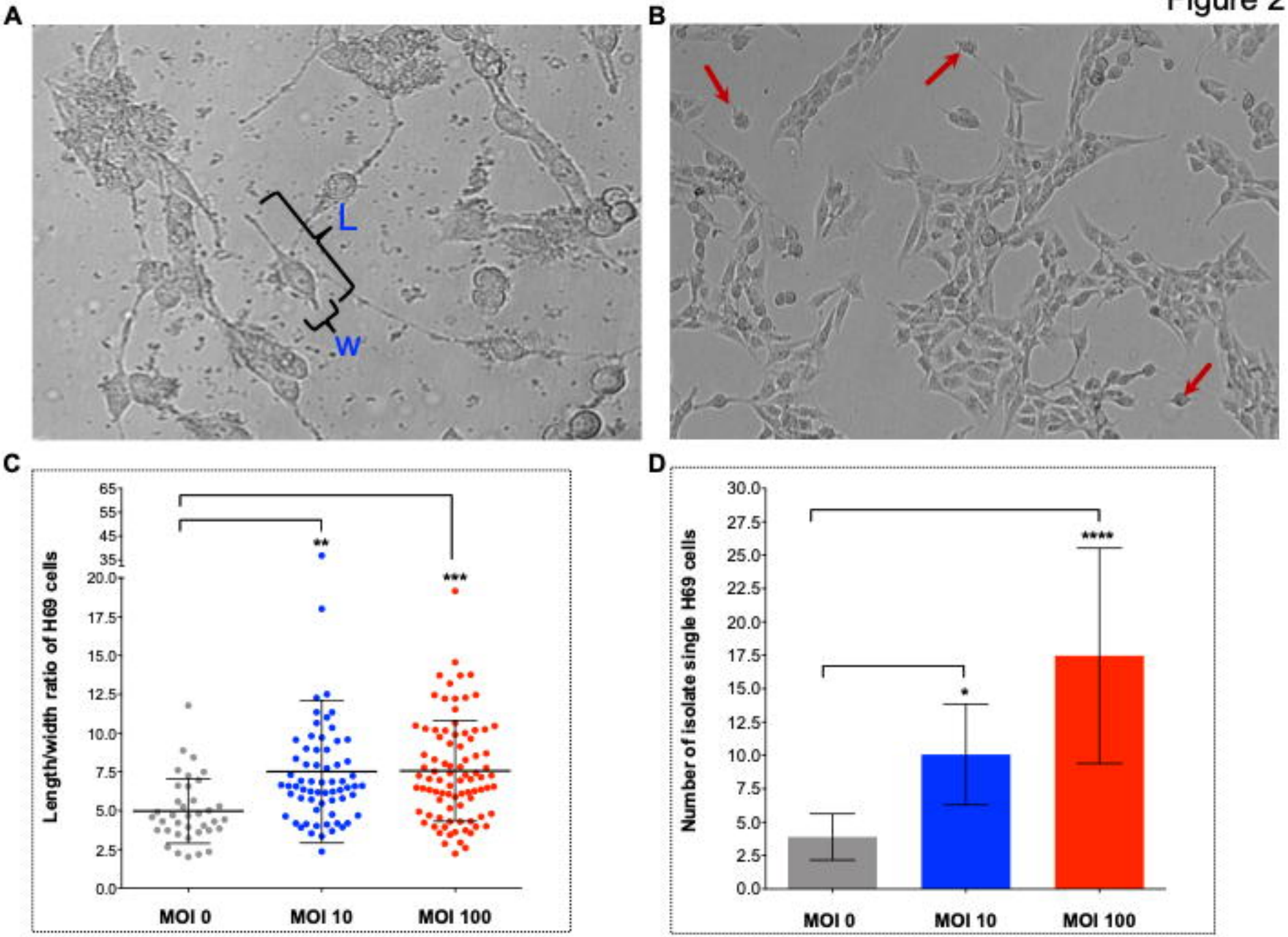
A
L
W
B
C
Length/width ratio of H69 cells
65
55
45
35
20.0
17.5
15.0
12.5
10.0
7.5
5.0
2.5
0.0
**
***
MOI 0
MOI 10
MOI 100
D
Number of isolate single H69 cells
30.0
27.5
25.0
22.5
20.0
17.5
15.0
12.5
10.0
7.5
5.0
2.5
0.0
*
****
MOI 0
MOI 10
MOI 100

Figure 3

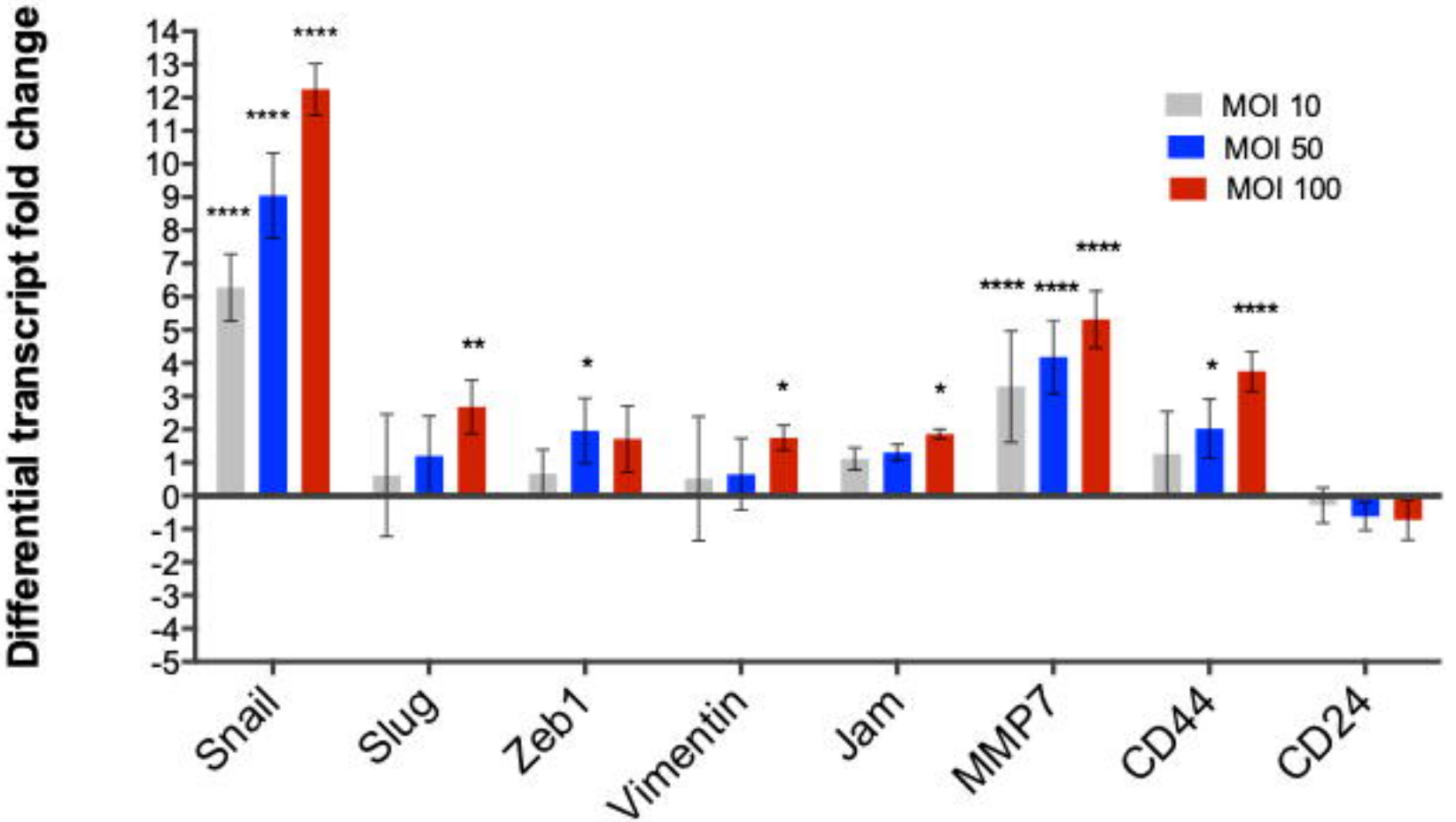
Differential transcript fold change
14
13
12
11
10
9
8
7
6
5
4
3
2
1
0
-1
-2
-3
-4
-5
MOI 10
MOI 50
MOI 100
****
****
****
**
*
*
*
****
****
****
*
****
Snail
Slug
Zeb1
Vimentin
Jam
MMP7
CD44
CD24

Figure 4

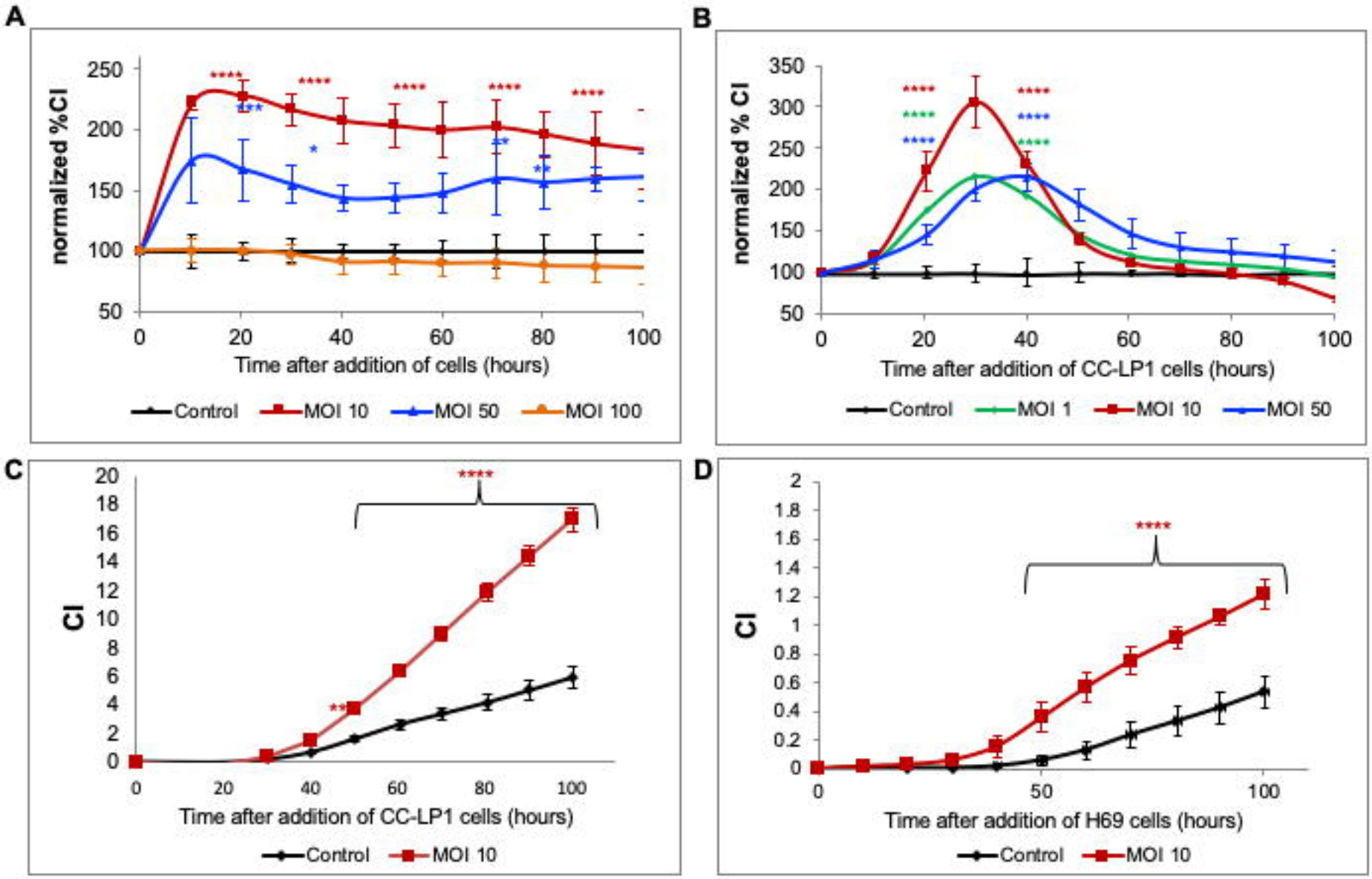
A
normalized %CI
250
200
150
100
50
0
20
40
60
80
100
Time after addition of cells (hours)
Control
MOI 10
MOI 50
MOI 100
B
normalized % CI
350
300
250
200
150
100
50
Time after addition of CC-LP1 cells (hours)
Control
MOI 1
MOI 10
MOI 50
C
CI
20
18
16
14
12
10
8
6
4
2
0
Time after addition of CC-LP1 cells (hours)
Control
MOI 10
D
CI
2
1.8
1.6
1.4
1.2
1
0.8
0.6
0.4
0.2
0
50
100
Time after addition of H69 cells (hours)
Control
MOI 10

Figure 5

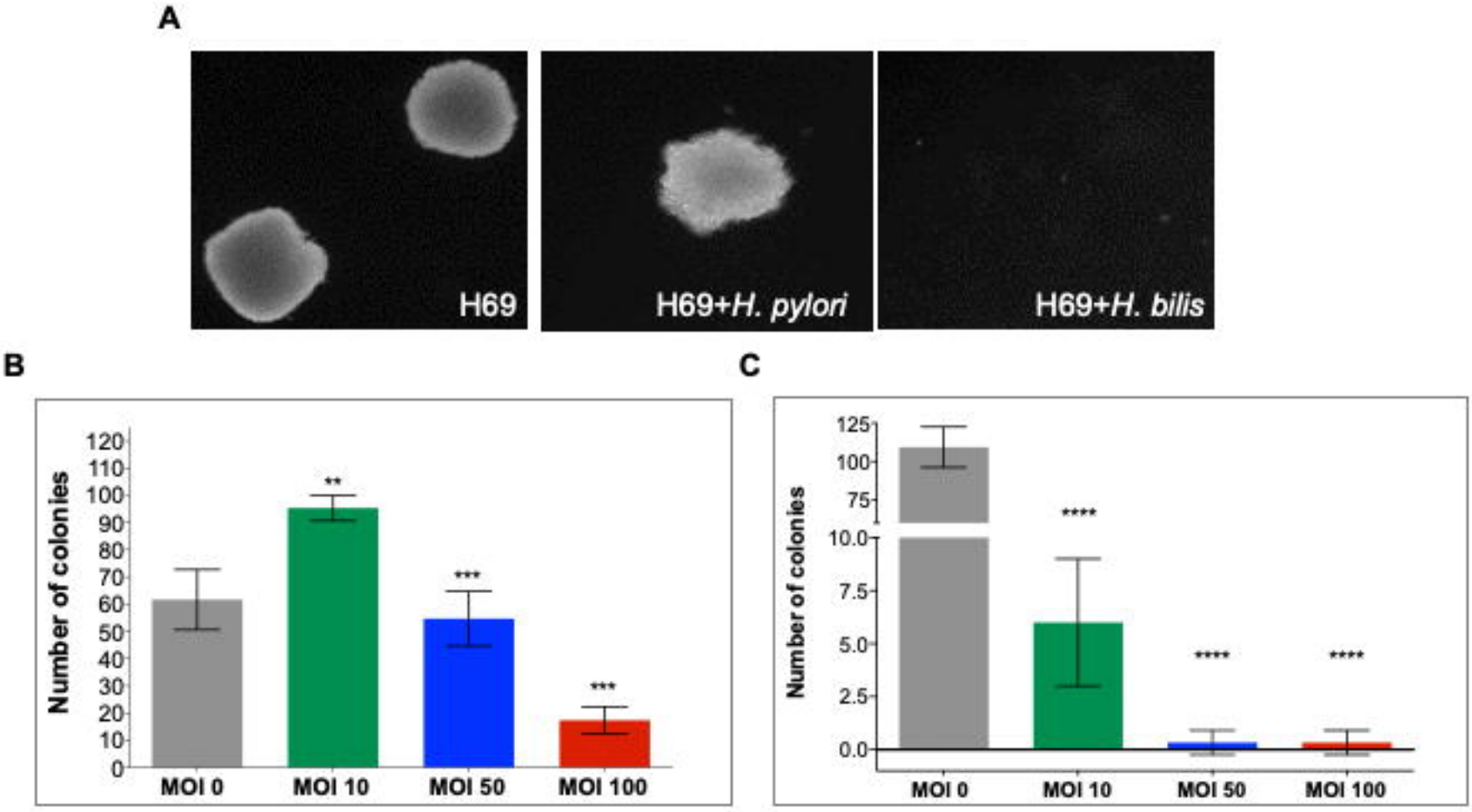
A
H69
H69+H. pylori
H69+H. bilis
B
Number of colonies
120
110
100
90
80
70
60
50
40
30
20
10
0
**
***
***
MOI 0
MOI 10
MOI 50
MOI 100
C
Number of colonies
125
100
75
10.0
7.5
5.0
2.5
0.0
****
****
****
MOI 0
MOI 10
MOI 50
MOI 100

Supplementary figure 1

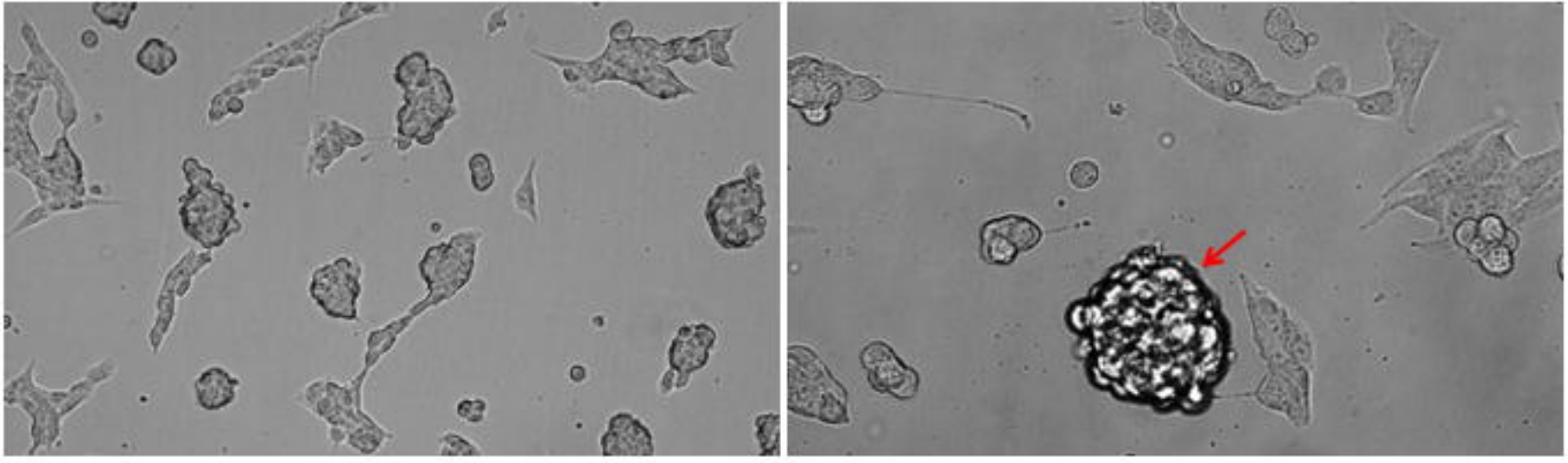

Supplementary figure 2

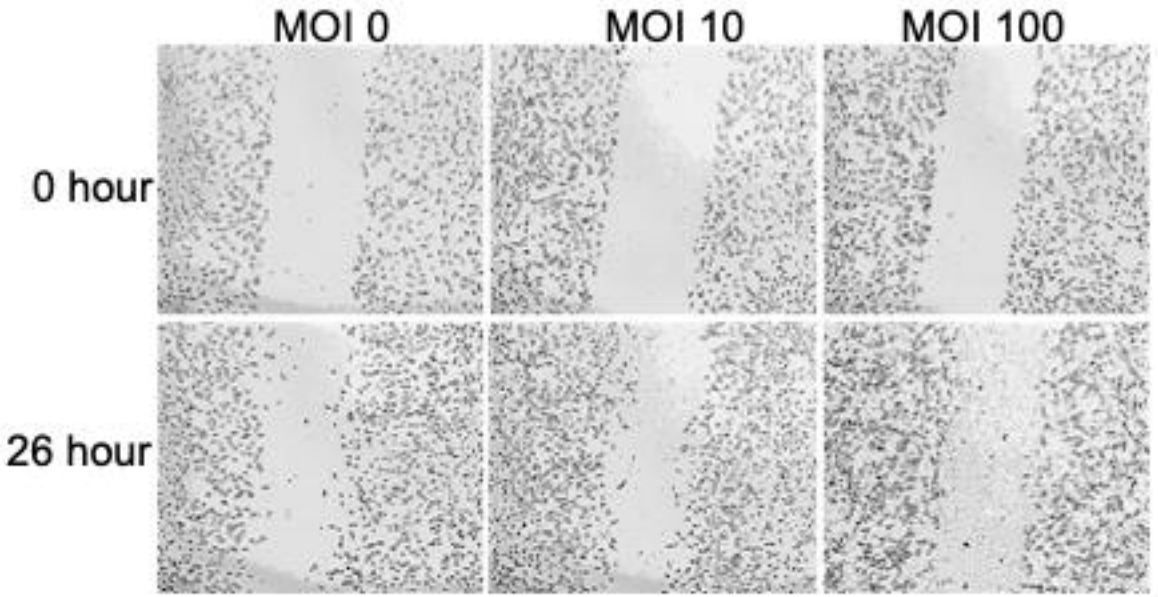

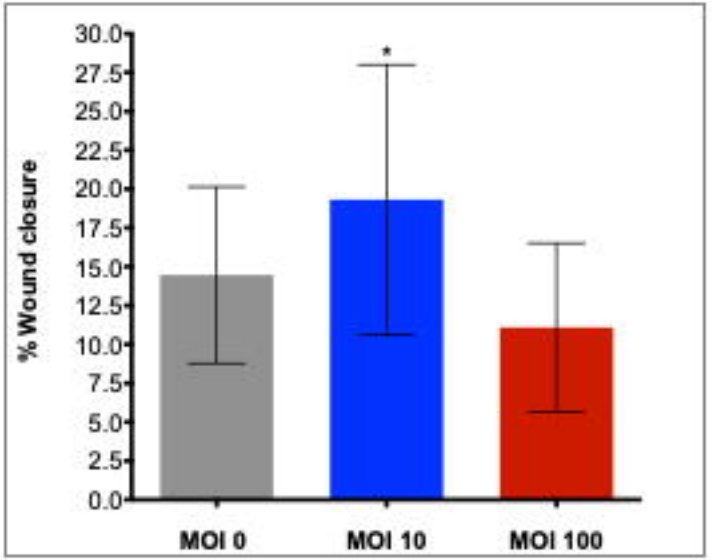

Supplementary figure 3

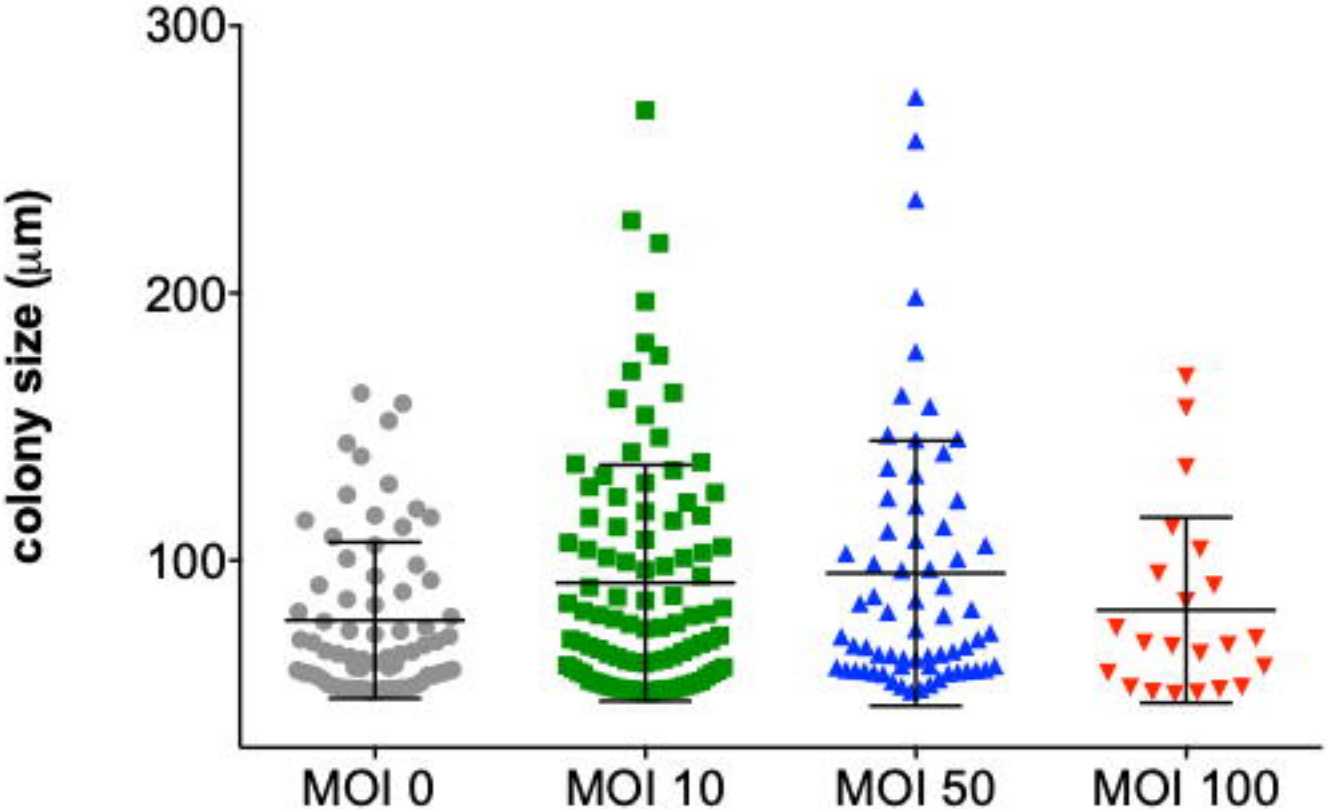
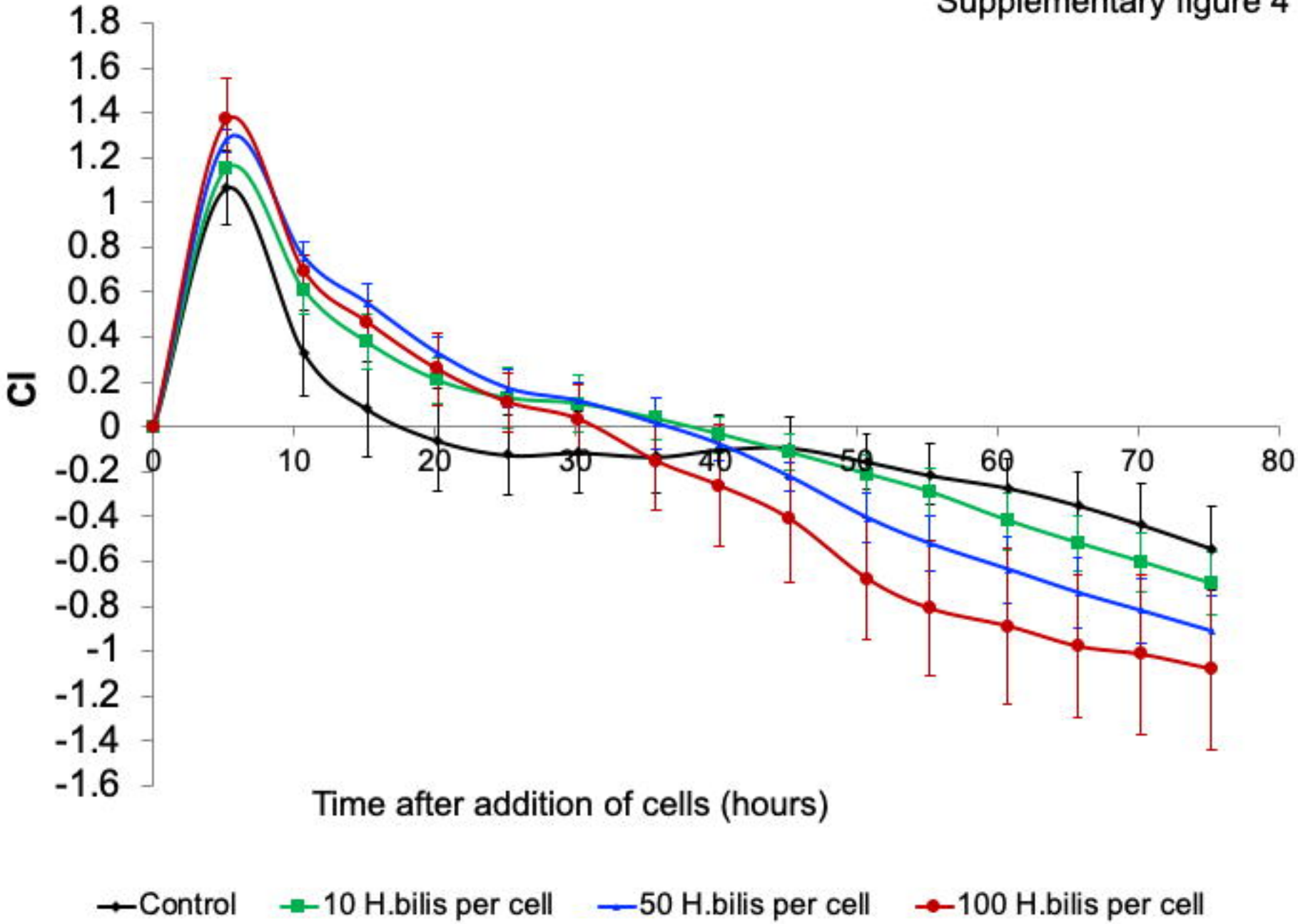
Supplementary figure 4